PHILOSOPHICAL TRANSACTIONS OF THE ROYAL SOCIETY A

Phil. Trans. R. Soc. A (2008) **366**, 591–607
doi:10.1098/rsta.2007.2112
Published online 13 August 2007

Wind direction modelling using multiple observation points

By Yoshito Hirata[1,2,3,*], Danilo P. Mandic[4], Hideyuki Suzuki[1,3] and Kazuyuki Aihara[1,2,3]

[1]*Department of Mathematical Informatics, The University of Tokyo, 7-3-1 Hongo, Bunkyo-ku, Tokyo 113-8656, Japan*
[2]*Aihara Complexity Modelling Project, ERATO, JST, 3-23-5-201 Uehara, Shibuya-ku, Tokyo 151-0064, Japan*
[3]*Institute of Industrial Science, The University of Tokyo, 4-6-1 Komaba, Meguro-ku, Tokyo 153-8505, Japan*
[4]*Department of Electrical and Electronic Engineering, Imperial College London, London SW7 2BT, UK*

The prediction of wind direction is a prerequisite for the intelligent and efficient operation of wind turbines. This is a complex task, due to the intermittent behaviour of wind, its non-Gaussian and nonlinear nature, and the coupling between the wind speed and direction. To provide improved wind direction forecasting, we propose a nonlinear model with augmented information from an additional measurement point. This is further enhanced by making use of both the speed and direction components of the wind field vector. The analysis and a comprehensive set of simulations demonstrate that the proposed approach achieves improved prediction performance over the standard and persistent model. The potential of the proposed approach is justified by the fact that even relatively small improvements in the forecasts result in large gains in the produced output power.

Keywords: chaos engineering; wind forecasting; multiple measurements; spatial correlation; experimental chaos; wind direction

1. Introduction and motivation

Wind farm technology has played a part in electricity production for more than a decade and is currently booming due to the global tendency to employ renewable power sources. Indeed, governments of several developed countries have set targets to increase the contribution of renewable sources up to 20% within the next 20 years. Of all the renewable energy sources, wind is perhaps most attractive, since it comes at no production or storage cost; the costs of the production and maintenance of wind turbines (WTs), however, are still rather prohibitive for large-scale deployment of this technology.

* Author and address for correspondence: Aihara Lab, Institute of Industrial Science, University of Tokyo, 4-6-1 Komaba, Meguro-ku, Tokyo 153-8505, Japan (yoshito@sat.t.u-tokyo.ac.jp).

One contribution of 14 to a Theme Issue 'Experimental chaos II'.

Owing to the intermittent nature of wind, and thus a relatively conservative fashion in which wind farms are operated, at present WTs do not take the maximum out of the available wind potential. Wind energy manufacturers usually recommend shutting off wind turbines if the wind conditions are considered to have high speed and large dynamics, which are capable of damaging the turbine. In addition, the WTs are not turned on at rather mild winds, since it is difficult to incorporate these power levels into the electricity grid.

The present mode of operation of WTs and wind farms (WFs) is therefore rather restricted. Wind turbines are normally located so as to face the direction of most frequent winds, and due to the distributed and frequency-sensitive nature of the grid, such energy is taken into the grid under stringent constraints. For example, energy providers commit to certain levels of service, and in order to incorporate the wind produced energy, they would have to reduce the input from, say, gas and oil operated power plants. Owing to the long times needed to cool down such power plants and to heat up the vapour again in order to continue energy production, WFs have been mostly used on small scales, when the weather forecasts firmly confirm large and long-lasting wind fronts. The medium- and long-time weather forecasts used are made using numerical weather forecasting (NWF) techniques based on models of the global movements of the atmosphere (for instance satellite aided).

Despite the importance of these global weather forecasts, it was also realized that the modelling of power output in wind turbines needs to be performed locally and in a real-time adaptive fashion. Although the NWFs are quite accurate, they are designed to model large atmospheric movements; the wind activity at a specific site has to be modelled locally and in a statistical manner (Kantz *et al.* 2004*a*,*b*).

WFs can be considered as a distributed network of sources, and the integration of such power into the grid ought to be performed in a predictive manner, based on robust short-term power estimates. Further, real-time control of wind generators and real-time vibration control need to be performed in a real-time adaptive way. Although both the output power of a WT and the control mechanism are directly dependent on wind, it is only recently that the modelling of wind has been recognized as a prerequisite for robust and reliable modelling and control within WFs (Roulston *et al.* 2003); this also highlights the need for the development of new algorithms for short-term wind forecasting. Indeed, short-term wind modelling has recently received much attention both in Europe and Japan (Ragwitz & Kantz 2000; Manwell *et al.* 2002; Roulston *et al.* 2003; Goh & Mandic 2004, 2005; Kantz *et al.* 2004*a*,*b*; Goh *et al.* 2006; Hirata *et al.* 2006*a*,*b*).

Given that a WF ought to operate in an intelligent, real-time adaptive manner, we set out to investigate whether efficient and local wind direction modelling would help towards this goal. Indeed, there are three major reasons for employing prediction and forecasting at different scales within an intelligent wind farm operation framework, which are the following.

(i) To predict the expected production of electricity (Roulston *et al.* 2003; Goh & Mandic 2004, 2005; Goh *et al.* 2006); for large WFs, this is typically achieved by using medium-range weather forecasts (Roulston *et al.* 2003). On a small scale, this is achieved based on historical data; this is also in line with current trends in microwind turbines for home use.

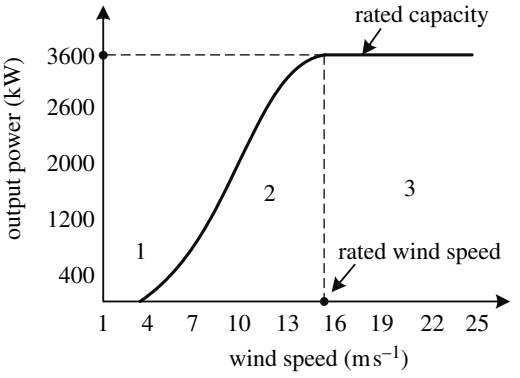

Figure 1. Power curve of a wind turbine. Region 1 with low wind speeds corresponds to no power production by a WT; region 2 is the operation region; in region 3, for high winds, the power output is subject to a threshold and ultimately the operation of a WT is stopped for high winds.

(ii) To avoid damages to wind turbines caused by gusts (Ragwitz & Kantz 2000; Kantz *et al.* 2004*a*,*b*); this is usually achieved based on a combination of short-term wind modelling and some sort of finite state machine.
(iii) To improve the efficiency of a WF and increase the power produced; this is achieved by adjusting the yaw of the blades and the direction of WTs so as to face the direction of the wind. It is now accepted that this should be performed based solely on the modelling of the wind field (speed and direction), since the output power of a WT is proportional to the cube of the incident wind speed.

In this paper, we focus on the third purpose. The proposed approach is also general enough to help with topics (i) and (ii) above; our analysis and simulations will therefore be conducted in a short-term prediction setting.

(*a*) *Wind production model*

It is nowadays widely accepted that in order to generate more electricity from a wind turbine, we need to predict the wind direction and consequently adjust the parameters of the wind turbine. Let us first introduce some parameters of wind turbines: let P denote the expected power output, ρ is the air density, C is the performance coefficient, parameter A is the area swept by the rotor and u is the wind speed perpendicular to the face of the rotor. The relation between the wind speed and the expected power output is given by Manwell *et al.* (2002)

$$P = \tfrac{1}{2}\rho C A u^3. \tag{1.1}$$

Since there is a cut-off wind speed in the actual WT operations for avoiding damages to WTs, the relation between the wind speed and the actual power output looks like that illustrated in figure 1. This relation as such gives only a ballpark figure and is not always applicable; for instance, the rotor does not always face the wind. This is, however, used as a standard in WT modelling, since the turbines are generally built to face the most prominent wind direction. In practice, the wind is coming from a much wider range of directions as

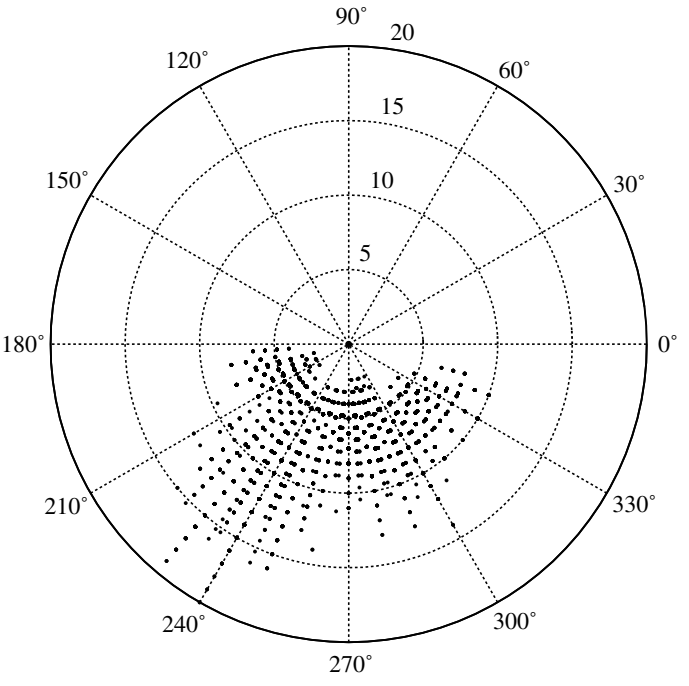

Figure 2. Wind rose: directional distribution of wind for a coastal site (Goh *et al.* 2006). The dataset for generating this graph was obtained from http://mesonet.agron.iastate.edu/request/awos/1min.php.

illustrated in figure 2. In order to achieve the real-time adaptivity and intelligent operation of WFs, we need to have more accurate estimates of P. To that end, a simple extension of equation (1.1) would be to assume that the wind direction and the vector normal to the face of rotor are at an angle θ, thus having $u = v\cos\theta$, where v denotes the absolute wind speed. In this way, equation (1.1) can be rewritten as

$$P = \tfrac{1}{2}\rho C A c^3 v^3 \cos^3\theta. \tag{1.2}$$

Observe that for $\theta = 20°$, the expected output power is 83% of the maximum given in equation (1.1); for $\theta = 45°$, this figure is 35%.

From figure 2 and equation (1.2), and since we cannot control the wind speed (although we can predict it), the modelling and forecasting of the wind direction is a prerequisite towards an intelligent operation of a WT and WF, a focus of this work. Yet, the current control approach is based on the adjustment to the direction of rotor after the wind direction has remained fixed for more than 10 min; this approach does not exploit all the available potential of wind and is not robust enough for the reliable control of a WT.

Recall also that wind is an intermittent phenomenon exhibiting strong non-Gaussianity, yet the available approaches to wind modelling are based on linear models. Our aim is therefore to introduce a general methodology for wind direction modelling, which will allow for a more proactive operation of WTs. Our focus is to investigate whether wind forecasting based on nonlinear models has advantages over linear approaches. This is a natural question due to the close relationship between non-Gaussianity and data nonlinearity (Gautama *et al.* 2004).

In addition, characteristic wind patterns, such as gusts, microbursts and turbulence, are conveniently analysed in an applied chaos framework which is inherently nonlinear; some recent results can be found in Goh *et al.* (2006). Simulations on real-world wind data support the approach.

2. Wind intermittency, sufficient information and experimental chaos

An important origin of chaos theory was the seminal work by Lorenz (1963), who analysed weather patterns. Subsequently, applications of chaos theory have been developed (Aihara & Katayama 1995; Aihara 2002). In particular, several approaches have analysed wind in the framework of nonlinear time series (Kantz & Schreiber 2003) and chaos (Kantz *et al.* 2004*b*).

Despite the mathematical elegance, it was soon realized that chaos is not readily applicable to real-world phenomena, which are prone to noise, uncertainty and time-varying statistics. Rejecting chaos totally as a framework for the analysis of real-world signals would be wrong; it has led to the development of chaos engineering and chaos-inspired real-world concepts such as those of bio-chaos and chaotic neuron (Aihara 2002).

Observe from figure 2, the coupling between the wind speed and direction components and recall the intermittent and hence non-Gaussian and nonlinear[1] nature of wind. It is in fact natural to consider wind modelling on short scales within the framework of *experimental chaos*,[2] given that characteristic wind episodes such as turbulence, microbursts and gusts, exhibit some sort of regularity in phase space.

Before proceeding with the analysis of wind prediction strategies, let us address some statistical properties of wind. Following the approaches from Hirata *et al.* (2004, 2005, 2007) and Goh *et al.* (2006), our findings show that:

(i) wind measurements considered as a time series have serial dependence (Hirata *et al.* 2005, 2007); this clearly justifies the modelling of such data within the framework of nonlinear regression and
(ii) depending on the wind regime and degree of averaging, wind time series may exhibit various degrees of nonlinear behaviour (Hirata *et al.* 2005; Goh *et al.* 2006).

Despite being somewhat inconclusive, these results provide evidence that wind is predictable on both the short and long scales.

From figure 2 and a number of our own experiments (Hirata *et al.* 2005), it was established that wind as a phenomenon is spatially local and temporally correlated, and that the components of such a signal are coupled. For instance, in figure 2, the highest wind speeds are recorded around the angle of 240°, whereas for the directions in the range between −70° and 210° there is hardly any wind activity.

[1] For more detail on the of signals in terms of their nonlinearity, see Gautama *et al.* (2003, 2004).
[2] Wind data are usually sampled with high sampling rate and then averaged to suit the needs of long-term wind forecasting. By averaging, the non-Gaussian nature of wind and hence nonlinearity are largely being lost. It therefore only makes sense to consider the raw, finely sampled wind data within the framework of experimental chaos, that is, in the applications of short term on-line adaptive wind modelling.

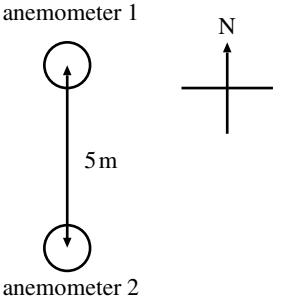

Figure 3. Observation set-up.

It is therefore natural to ask ourselves what would be a 'sufficient information' or 'sufficient statistics', that is what would be the span of temporal regression (memory) and spatial dimension (degrees of freedom) for such data.

A series of our earlier results, both in terms of applied chaos and nonlinear signal processing, have illustrated that

— it is not possible to predict the wind profile sufficiently well using only observations at one measured point; and
— it is possible to improve wind forecasts if there is at least one more measured point upwind from the original one.

To date, it is unclear the extent to which the use of a nonlinear forecasting model and multiple measurement points improves the prediction. We shall therefore focus on the problem of wind direction forecasting based on observations from two different measurement points.

3. Predicting the wind direction using two observation points

The so-called *persistent* model is a de facto standard in WF operation, whereby it is assumed that the predicted wind speed will be the same as the current speed (zeroth-order model). It is therefore our initial aim to establish whether the nonlinear prediction of wind based on two observations taken at separate points provides better prediction performance as compared to the persistent prediction.

(*a*) *Observation set-up*

The data analysed were wind data observed over 24 hours, on 24 October 2005, starting from 14.00. The experiment was conducted in an urban environment at the Institute of Industrial Science, The University of Tokyo. Two matched ultrasonic anemometers were used, which were located along the north–south axis and located 5 m apart, as illustrated in figure 3. The wind measurements were three-dimensional and sampled at 50 Hz, that is, in the east–west, north–south and upward–downward directions. This particular setting was used in order to simulate a 1/100 scale of an actual wind farm.

For the preprocessing of the data, a moving average filter on 2 s windows was used, the data were then resampled at 2 s intervals. For convenience, we ignored the upward–downward direction and conducted our analysis only in the plane spanned by the east–west and north–south direction.

Figure 4 and table 1 provide a comprehensive account of the statistics for the 24 hours of wind data considered. Both quantitative and qualitative measures describing such a process (including spatial distributions) are illustrated.

Figure 4*a* illustrates wind as a vector field, described by its speed and direction. Alternatively, we can base our modelling on the projections of this vector on the north and east axes. The representation for wind also depends on the way wind data are recorded: standard cup anemometers provide the speed–direction information, whereas modern ultrasonic instruments have a much wider range of options. This is illustrated in figure 4*b*, where by inspection, wind was relatively strong in the intervals between 14.00 and 16.00; 22.00 and 02.00; and 10.00 and 14.00 (figure 4*b*(i)(ii)). As for the wind direction, figure 4*b*(iii) shows that between 22.00 and 02.00 and between 10.00 and 14.00, the dominant wind direction was from the north, whereas between 14.00 and 16.00, the dominant wind direction was from the south.

A more convenient way to visualize these four time series is shown in figure 4*c*, in the form of wind lattice (wind rose similar to figure 2), where for every time instant the tip of the wind vector is represented by a dot. Observe a clear coupling between strong winds and the north–south direction. To further depict the range of wind directions, the histogram of figure 4*d* exhibits two peaks: the peak associated with the easterly wind is related to the quiet periods between 18.00 and 22.00 and between 02.00 and 10.00. The peak related to the northerly wind is related to high winds between 22.00 and 02.00 and between 10.00 and 14.00.

The autocorrelation based on the increments of wind direction from figure 4*e* shows anticorrelation at a lag between 2 and 6 s. Owing to the experiment having been conducted in an urban environment, for approximately 40% of the measured time, the wind speed was rather low and in the range between 0 and 0.2 m s^{-1} as shown in the histogram in figure 4*f*. The variation of the wind speed showed large fluctuations since the mean speed and its standard deviation were almost equal (table 1).

From the above analysis, it is clear that it is the forecasting of the wind direction that will have a major contribution in the intelligent operation of a WT. Since our underlying aim is to predict the wind direction, a straightforward approach would be to construct a prediction model based on the past values of the wind direction only. However, since wind speed and direction are coupled, our proposed model will take advantage of the available wind speed information, in order to predict direction only. The schematic graph is shown in figure 5. This task may be considered within the framework of experimental chaos. In fact, the embedding parameters and the different wind dynamics have been analysed in our previous work (Goh *et al.* 2006).

Let $y_{1,1}(t)$ and $y_{1,2}(t)$ be the wind direction and speed at time t for anemometer 1 (A1) and $y_{2,1}(t)$ and $y_{2,2}(t)$ those for anemometer 2 (A2), and let us consider a model that predicts the future wind direction at A2 based on the observed wind direction and speed from both the north and south (A1 and A2), as illustrated in figure 3. Based on an extension of the approach proposed by Judd and Mees (Hirata *et al.* 2006*b*), the maximum delay of 60 s was used for each element of y; the initial 'optimal' set $z(t)$ of such delays used in the prediction can therefore be

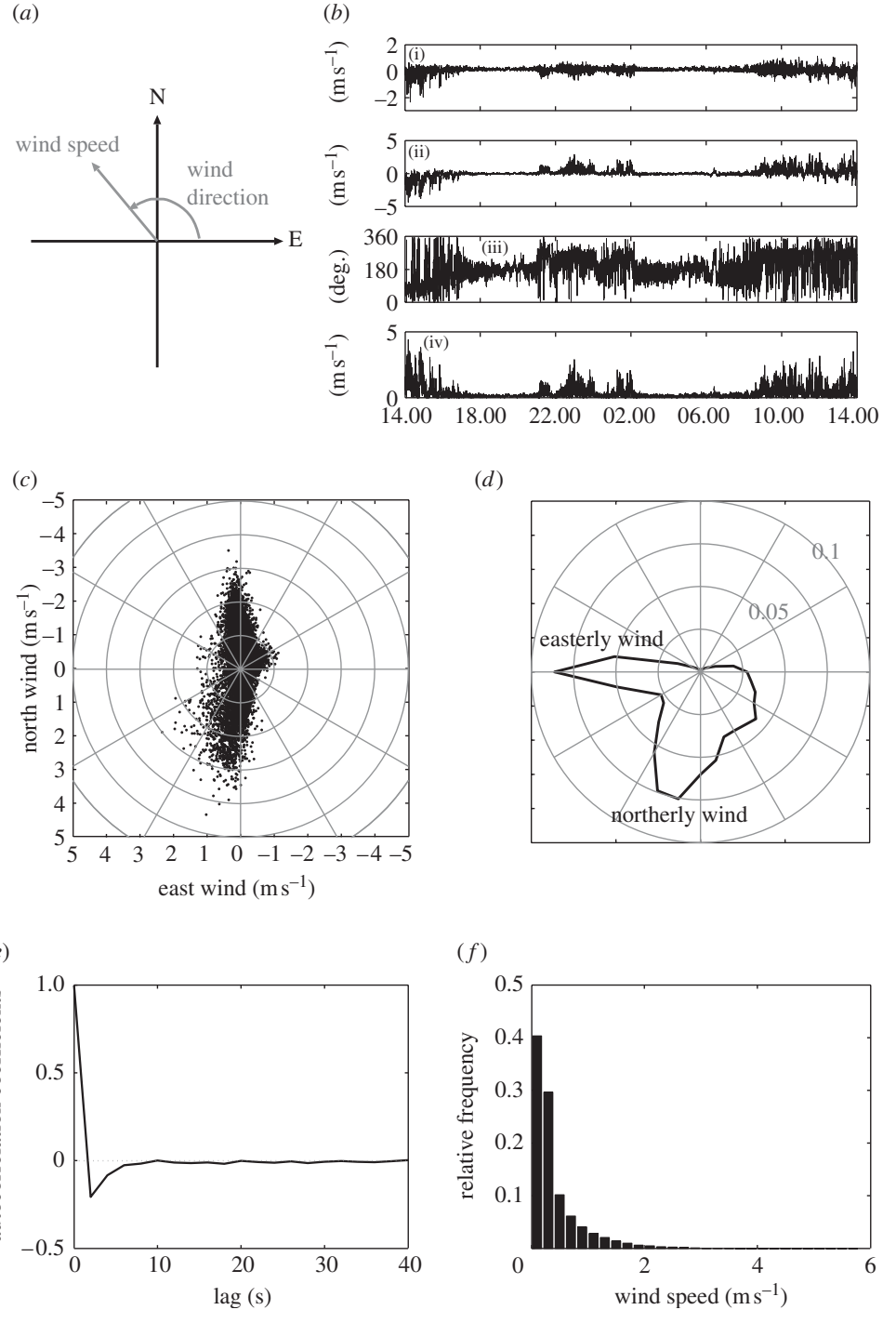

Figure 4. Quantitative and qualitative wind descriptors: (*a*) wind vector representation, (*b*(i)) time series of the easterly wind, (ii) northerly wind, (iii) wind direction and (iv) wind speed, (*c*) wind rose representation, (*d*) relative frequencies for wind direction, (*e*) autocorrelation based on increments of wind direction of 2 s and (*f*) relative frequencies calculated for wind speed.

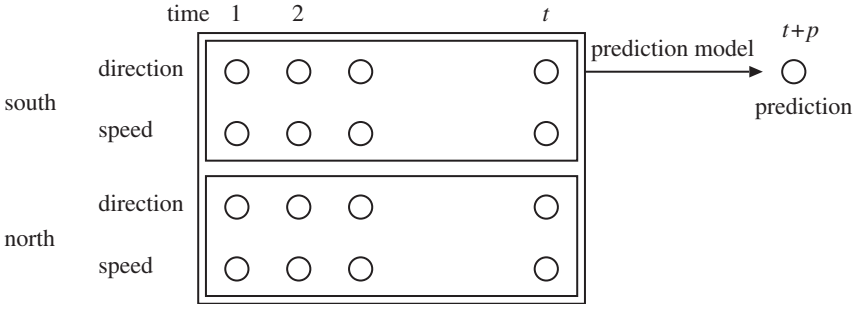

Figure 5. Illustration of the direction–speed model.

Table 1. Statistical properties of the dataset.

minimum speed	0 ($\mathrm{m\,s^{-1}}$)
maximum speed	5.25 ($\mathrm{m\,s^{-1}}$)
mean speed	0.41 ($\mathrm{m\,s^{-1}}$)
standard deviation of speed	0.44 ($\mathrm{m\,s^{-1}}$)

expressed as

$$\begin{aligned} z(t) = (&y_{1,1}(t-\tau_{1,1,1}), y_{1,1}(t-\tau_{1,1,2}), \ldots, y_{1,1}(t-\tau_{1,1,k_{1,1}}),\\ &y_{1,2}(t-\tau_{1,2,1}), y_{1,2}(t-\tau_{1,2,2}), \ldots, y_{1,2}(t-\tau_{1,2,k_{1,2}}),\\ &y_{2,1}(t-\tau_{2,1,1}), y_{2,1}(t-\tau_{2,1,2}), \ldots, y_{2,1}(t-\tau_{2,1,k_{2,1}}),\\ &y_{2,2}(t-\tau_{2,2,1}), y_{2,2}(t-\tau_{2,2,2}), \ldots, y_{2,2}(t-\tau_{2,2,k_{2,2}})). \end{aligned} \tag{3.1}$$

To facilitate the nonlinear mode of operation, we next investigate an affine+radial basis function model with 100 radial basis functions as proposed by Judd & Mees (1995) with the normalized maximum likelihood (Rissanen 2000) as the information criterion.

There are two basic ways of multiple step ahead prediction: the direct and iterated mode, where the iterated mode suits feedback prediction models. Owing to the choice of our computing model, we used direct predictions, for which p step ahead prediction model has the form of

$$y_{2,1}(t+p) \approx f_p(z(t)) = a_p + b_p \cdot z(t) + \sum_{j=1}^{100} c_{p,j} \exp\left(-\frac{||z(t)-d_{p,j}||^2}{2\sigma_p^2}\right), \tag{3.2}$$

where a_p, b_p, $c_{p,j}$, $d_{p,j}$ and σ_p are parameters of the model.

In the model evaluation set-up, the performance of the proposed direction–speed model was compared to that of a persistent model, for which the wind direction at 2 s before the actual point of interest was used as a persistent prediction.

Our proposed model was built based upon the first 2000 points of the data and the performance was evaluated on the subsequent 200 data points. To cover all the available data, these data windows were shifted by 200 points after every prediction and this process was repeated for 206 times.

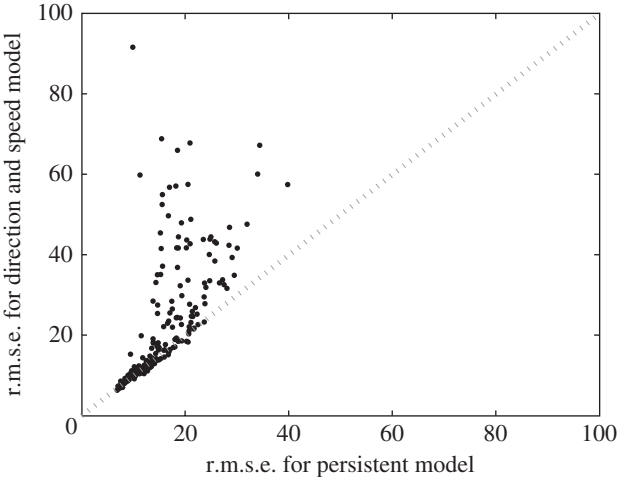

Figure 6. Scatter diagram illustrating the performance of the persistent and direction–speed model for a one step ahead prediction task. Each point corresponds to a prediction window. The horizontal axis is the root mean square error (r.m.s.e.) for the persistent model and the vertical axis corresponds to the r.m.s.e. for the direction–speed model. This way, if the r.m.s.e. for the persistent model is smaller than that for direction–speed model, the resulting point in the scatter diagram will be above the bisector line.

The performance comparison shown in figure 6 shows that for this rather raw case, the persistent model exhibited better performance than the proposed direction–speed model. This result may be explained by the fact that the direction signal has a circular nature, hence experiencing problems around the singular points, where such prediction is totally unreliable.

(*b*) *The two-dimensional model*

To overcome the problem with the discontinuity associated with a circular nature of wind direction, we propose a two-dimensional model, whereby the winds coming from east and north were predicted at the south anemometer and then the wind directions were calculated from these predictions. The predictions were based on the observations from both the south and north anemometer (figure 7). The procedures for making a predictive model were the same as those used in the speed–direction model. We found that the two-dimensional model was likely to be better than the persistent model as illustrated in figure 8*a*, where the majority of the points are located below the bisector line. This result is consistent with our previous study (Hirata *et al.* 2006*a*), where the observations from the predicted point only were used for the prediction. Even in the case of a 20 s ahead direct prediction, this tendency continued (figure 8*b*). Over all the tested intervals, the two-dimensional model showed tendency to have a smaller prediction error than the persistent model. In figure 9, the probability that the two-dimensional model has a smaller prediction error than the persistent model is above 0.5 for all the tested prediction horizons, thus indicating superiority of the two-dimensional model over the persistent model. The direction–speed model exhibited worse performance than the persistent model when the prediction horizon was less than 5 s.

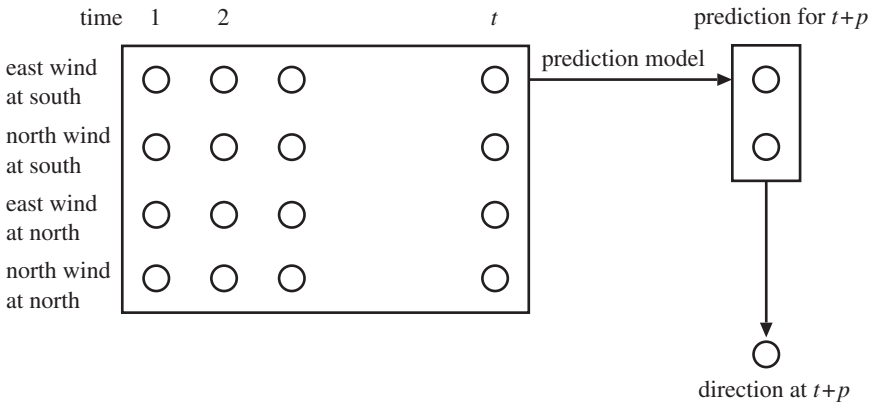

Figure 7. Block diagram of the proposed two-dimensional model.

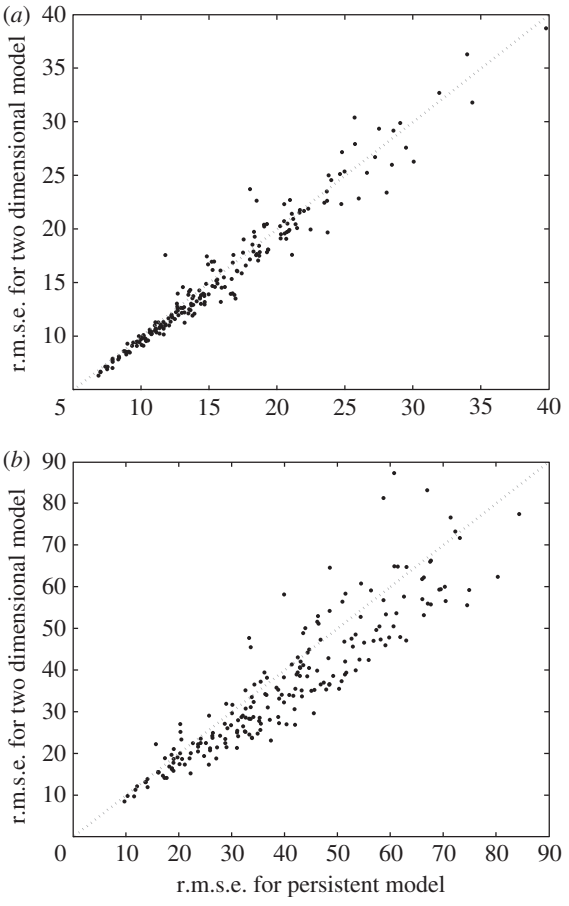

Figure 8. Performance of the two-dimensional model for (*a*) 2 s and (*b*) 20 s ahead prediction. The horizontal axis is the root mean square error (r.m.s.e.) for the persistent model and the vertical axis corresponds to the r.m.s.e. for the two-dimensional model. In both the figures, more points are located below the bisector line, indicating that the two-dimensional model showed better performance than the persistent model.

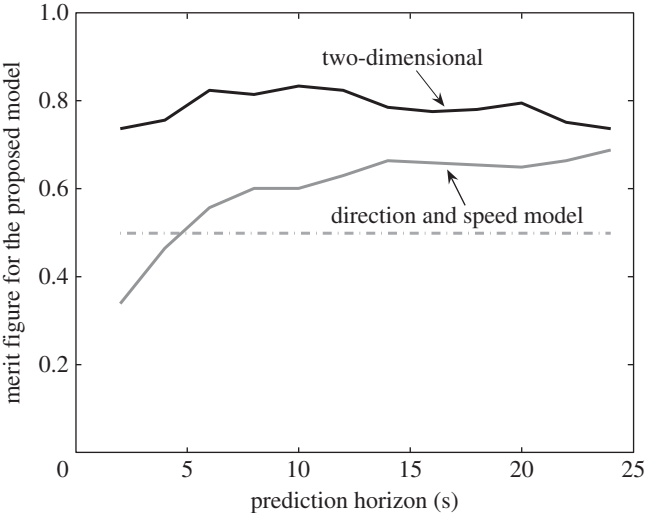

Figure 9. Comparison of the prediction performance between the proposed and persistent model. Letting m be the number of windows for which the prediction error is smaller than that of the persistent model and n the total number of windows, we calculated the ratio m/n for each prediction horizon.

4. Factors in the prediction of the wind direction

The performance of a prediction model heavily leans on the amount and spatial distribution of the data, number of observation points and the choice of model (linear and nonlinear).

(*a*) *Choice of the number of measurement points*

Closely related to the concept of data fusion and sufficient information (Mandic *et al.* 2007), we have gathered both the theoretical and empirical evidence that the prediction performance improved when measurements from two spatially distributed anemometers were used. Indeed, for the wind direction prediction experiment for the south anemometer, the additional information coming from the north anemometer improved the prediction error. This is illustrated in figure 10*a*, where the majority of the points are below the bisector line. On the other hand, when the wind direction at the north anemometer was predicted based on the measurements from the north and south anemometer, the second set of observations coming from the south point did not improve the prediction, as illustrated in figure 10*b*.

Over all the tested prediction intervals, the second observation coming from upwind enhanced the prediction: according to figure 11, when using additional observations upwind, the probability that the model using observations upwind has a smaller prediction error was always above 0.5. When observations from downwind were taken, the probability that the model using those observations has a smaller prediction error than that without them was approximately 0.5. It therefore did not make much difference whether the downwind observations were used.

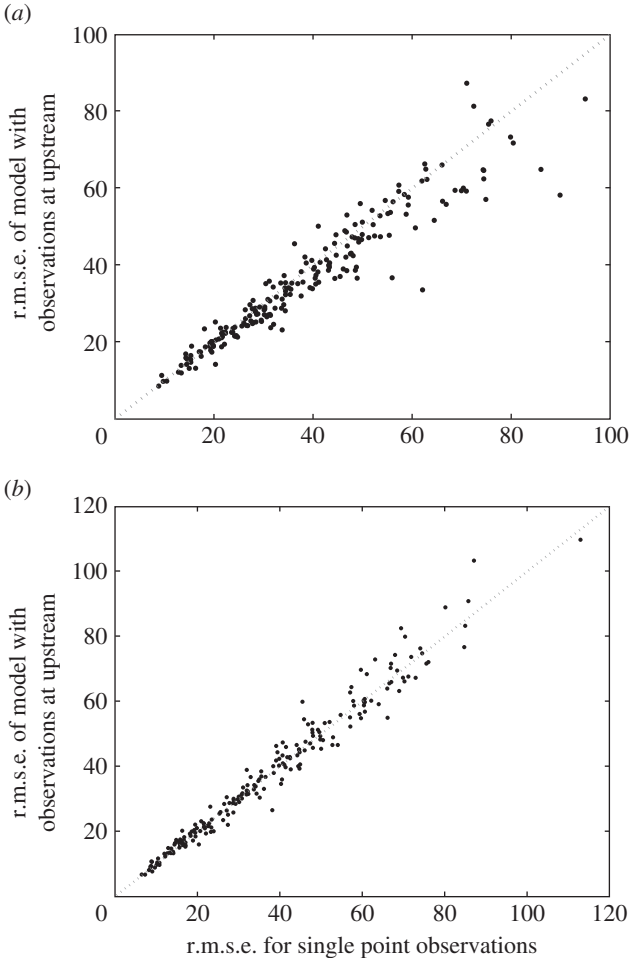

Figure 10. Wind direction prediction (20 s ahead) at the (*a*) south and (*b*) north points. (*a*) Extra observation point (north point) is upwind. (*b*) Extra observation point (south point) is downwind. In each figure, the horizontal axis is the root mean square error (r.m.s.e.) for the two-dimensional model based on the single observation point and the horizontal axis corresponds to the r.m.s.e. for the two-dimensional model based on the two observation points.

(*b*) *Nonlinear versus linear models*

The performance of our proposed nonlinear model was next compared against that of the linear model. The linear model, in the form of $a_p + b_p \cdot z(t)$, was used in the same simulation set-up as the nonlinear affine + radial basis function model.

The nonlinear model did not exhibit a significant difference in the performance over the linear model; this is illustrated in figure 12, where the points in the scatter diagram are distributed around the bisector line. The probability that for each prediction horizon the nonlinear model has a smaller prediction error than the linear model is shown in figure 13.

When predicting the wind direction 2 s ahead, we found that the nonlinear model was likely to be more suitable than the linear one, since when the wind direction was being predicted 2 s ahead, the probability that the prediction error

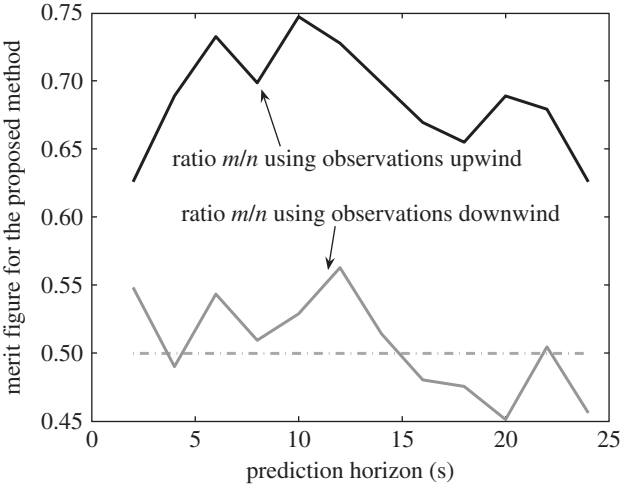

Figure 11. Comparison of the prediction performance between the two-dimensional model based on two observation points and that based on a single observation point. Letting m be the number of windows for which the prediction error for the model using observations upwind (downwind) is smaller than that obtained without them and n being the total number of windows, we calculated the ratio m/n for each prediction horizon.

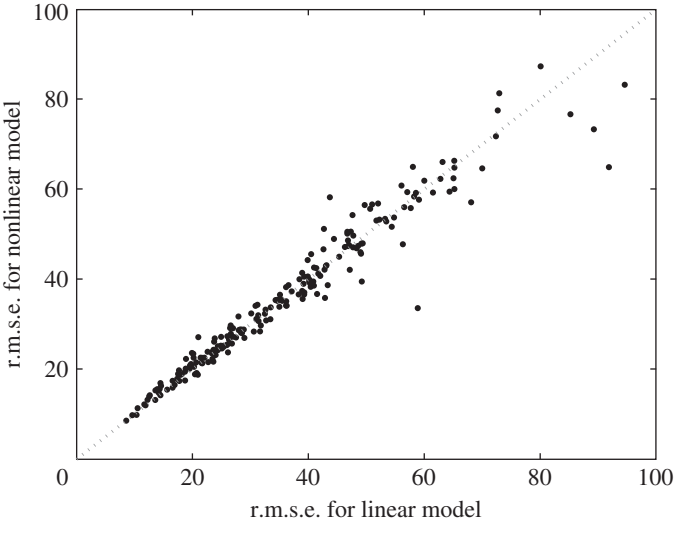

Figure 12. Comparison of the linear and nonlinear wind direction prediction models at the south point using our two-dimensional model and observations at both points (20 s ahead). The horizontal axis is the root mean square error (r.m.s.e.) of linear model and the vertical axis corresponds to the r.m.s.e. of nonlinear model.

for the nonlinear model was smaller than that for the linear model was above 0.5. This tendency was also observed in other datasets. In the short time ranges, the increments for the wind direction are anticorrelated (figure 4*e*) and the nonlinearity of the short-term prediction may be due to this anticorrelation.

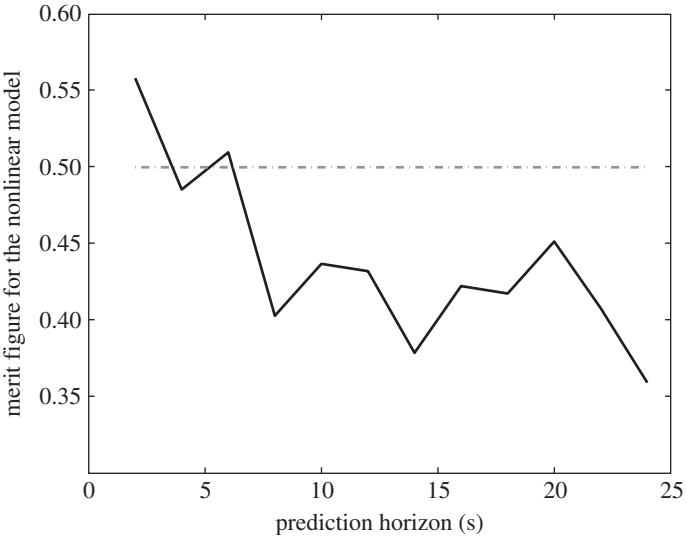

Figure 13. Comparison of the prediction performance between the nonlinear and linear model. Letting m be the number of windows for which the prediction error for the nonlinear model is smaller than that for the linear model and n the total number of windows, we calculated the ratio m/n for each prediction horizon.

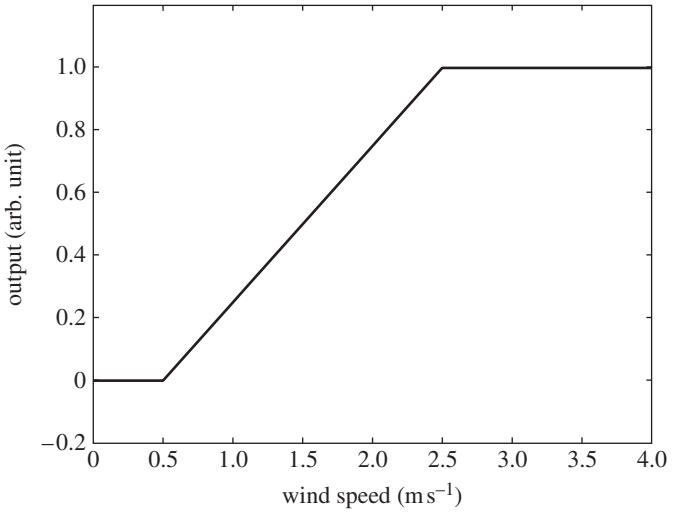

Figure 14. First approximation of the power curve from figure 1.

5. Benefits of the proposed nonlinear multiobservation model

Although the difference in the prediction errors between the two-dimensional and persistent model was small, this produced a significant difference in the expected electricity production. To quantify this, in the following simulation, we used the predicted wind directions and speeds for the control of a wind turbine and subsequently estimated the expected amount of produced electricity using the actual data. In the simulation, we used the simplified power curve given in figure 14.

Table 2. Expected electricity production from each combination of methods.

direction	speed	energy estimated (arb. unit)
speed–direction	speed–direction	1546.9
persistent	persistent	1608.7
two-dimensional	persistent	1611.3
persistent	two-dimensional	1690.2
two-dimensional	two-dimensional	1721.9

In this experiment, we also compared some existing methods, as shown in table 2 where when two-dimensional models were used for the modelling of wind directions and speeds, the improvement in the total amount of energy was 7% in the case when the persistent models were used for predicting the wind directions and speeds, and 2% in the case when using the persistent model for predicting the wind directions and the two-dimensional model for predicting wind speeds.

6. Conclusions

We have introduced a novel theoretical and experimental framework for the prediction of wind direction based on a two-dimensional wind vector representation. The benefits of the proposed approach are based on the use of two observation points which has led to the consistently improved performance as compared to the persistent model. Although the difference in quantitative performance between the proposed method and the persistent prediction is relatively small, this makes a significant difference in the expected production of electricity.

This study was partially supported by the Industrial Technology Research Grant Program in 2003, from the New Energy and Industrial Technology Development Organization (NEDO) of Japan. The work of D.P.M. was supported by EPSRC (EP/D061709/1).

References

Aihara, K. 2002 Chaos engineering and its application to parallel distributed processing with chaotic neural networks. *Proc. IEEE* **90**, 919–930. (doi:10.1109/JPROC.2002.1015014)

Aihara, K & Katayama, R. 1995 Chaos engineering in Japan. *Commun. ACM* **38**, 103–107. (doi:10.1145/219717.219801)

Gautama, T., Mandic, D. P. & Van Hulle, M. M. 2003 On the indications of nonlinear structures in brain electrical activity. *Phys. Rev. E* **67**, 046204. (doi:10.1103/PhysRevE.67.046204)

Gautama, T., Mandic, D. P. & Van Hulle, M. M. 2004 The delay vector variance method for detecting determinism and nonlinearity in time series. *Physica D* **190**, 167–176. (doi:10.1016/j.physd.2003.11.001)

Goh, S. L. & Mandic, D. P. 2004 A complex-valued RTRL algorithm for recurrent neural networks. *Neural Comput.* **16**, 2699–2713. (doi:10.1162/0899766042321779)

Goh, S. L. & Mandic, D. P. 2005 Nonlinear adaptive prediction of complex-valued signals by complex-valued PRNN. *IEEE Trans. Signal Process.* **53**, 1827–1836. (doi:10.1109/TSP.2005.845462)

Goh, S. L., Chen, M., Popović, D. H., Aihara, K., Obradovic, D. & Mandic, D. P. 2006 Complex-valued forecasting of wind profile. *Renew. Energ.* **31**, 1733–1750. (doi:10.1016/j.renene.2005.07.006)

Hirata, Y., Suzuki, H., Aihara, K., Abe, R., Kanie, K., Yamada, T. & Takahashi, J. 2004 Looking for nonlinearity in the dynamics of surface wind using surrogate data. In *Proc. 2004 Int. Symp. on Nonlinear Theory and its Applications (NOLTA 2004), Fukuoka, Japan, November 2004*, pp. 207–210.

Hirata, Y., Suzuki, H. & Aihara, K. 2005 Predicting the wind using spatial correlation. In *Proc. 2005 Int. Symp. on Nonlinear Theory and its Applications (NOLTA 2005), Bruges, Belgium, October 2005*, pp. 634–637.

Hirata, Y., Suzuki, H. & Aihara, K. 2006*a* Predicting wind direction using nonlinear models and time series data. In *2006 Annual Meeting Record I.E.E. Japan*, vol. 7, p. 87.

Hirata, Y., Suzuki, H. & Aihara, K. 2006*b* Reconstructing state spaces from multivariate data using variable delays. *Phys. Rev. E* **74**, 026202. (doi:10.1103/PhysRevE.74.026202)

Hirata, Y., Horai, S., Suzuki, H. & Aihara, K. 2007 Testing serial dependence by Random-shuffle surrogates and the Wayland method. *Phys. Lett. A* **370**, 265–274. (doi:10.1016/j.physleta.2007.05.061)

Judd, K. & Mees, A. 1995 On selecting models for nonlinear time series. *Physica D* **82**, 426–444. (doi:10.1016/0167-2789(95)00050-E)

Kantz, H. & Schreiber, T. 2003 *Nonlinear time series analysis*. Cambridge, UK: Cambridge University Press.

Kantz, H., Holstein, D., Ragwitz, M. & Vitanov, N. K. 2004*a* Markov chain model for turbulent wind speed data. *Physica A* **342**, 315–321. (doi:10.1016/j.physa.2004.01.070)

Kantz, H., Holstein, D., Ragwitz, M. & Vitanov, N. K. 2004*b* Extreme events in surface wind: predicting turbulent gusts. In *Proc. 8th Experimental Chaos Conference, Florence, Italy, 14–17 June 2004*, vol. 742 (ed. S. Boccaletti). AIP Conference Proceedings, pp. 315–324. New York, NY: American Institute of Physics.

Lorenz, E. N. 1963 Deterministic nonperiodic flow. *J. Atmos. Sci.* **26**, 130–141. (doi:10.1175/1520-0469(1963)020<0130:DNF>2.0.CO;2)

Mandic, D. P., Goh, S. L. & Aihara, K. 2007 Sequential data fusion via vector spaces: fusion of heterogeneous data in the complex domain. *Int. J. VLSI Signal Process. Syst.* **48**, 99–108. (doi:10.1007/s11265-006-0025-6)

Manwell, J. F., McGowan, J. G. & Rogers, A. L. 2002 *Wind energy explained: theory, design and application*. New York, NY: Wiley.

Ragwitz, M. & Kantz, H. 2000 Detecting non-linear structure and predicting turbulent gusts in surface wind velocities. *Europhys. Lett.* **51**, 595–601. (doi:10.1209/epl/i2000-00379-x)

Rissanen, J. 2000 MDL denoising. *IEEE Trans. Inform. Theory* **46**, 2537–2543. (doi:10.1109/18.887861)

Roulston, M. S., Kaplan, D. T., Hardenberg, J. & Smith, L. A. 2003 Using medium-range weather forecasts to improve the value of wind energy production. *Renew. Energ.* **28**, 585–602. (doi:10.1016/S0960-1481(02)00054-X)